Journal of Molecular Liquids 365 (2022) 120109

Contents lists available at ScienceDirect

Journal of Molecular Liquids

journal homepage: www.elsevier.com/locate/molliq

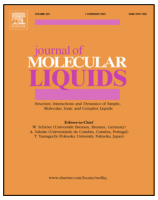

Dual liquid Crystalline/Gel behavior with AIE effect promoted by Self-assembly of pyrazole dendrons

Verónica Iguarbe [a], Pilar Romero [a], Joaquín Barberá [a], Anabel Elduque [b],*, Raquel Giménez [a],*

[a] Instituto de Nanociencia y Materiales de Aragón (INMA), Departamento de Química Orgánica, Facultad de Ciencias, CSIC-Universidad de Zaragoza, 50009 Zaragoza, Spain
[b] Instituto de Síntesis Química y Catálisis Homogénea (ISQCH), Departamento de Química Inorgánica, Facultad de Ciencias, CSIC-Universidad de Zaragoza, 50009 Zaragoza, Spain

ARTICLE INFO

Article history:
Received 31 May 2022
Revised 27 July 2022
Accepted 14 August 2022
Available online 18 August 2022

Keywords:
Dendrimers
Self-assembly
Liquid crystal
Gel
Luminescence
AIE
Hydrogen bond

ABSTRACT

This work describes the rich self-assembly behavior obtained by grafting a pyrazole-derived platform at the focal point of poly(benzyl ether) dendrons. Liquid crystals and supergels made out of fibers are obtained by supramolecular organization of non-discoid entities, and they notably increment the photoluminescence in these aggregated states (Aggregation-Induced Emission, AIE). The novel focal point, which is derived from 3,5-dimethyl-4-phenyl-1*H*-pyrazole, shows great tendency to arrange both wedge-shaped or cone-shaped dendrons in columnar arrangements by the formation of supramolecular polymers by hydrogen-bonding following the cylinder model. Two different linkers, amide or ether groups, connecting with the pyrazole-based apex are investigated, obtaining similar mesomorphic behavior, but different luminescent properties. A combined study of NMR, IR and X-ray diffraction allows establishing analogies between the fiber mesoscopic organization and the columnar organization in the liquid crystalline phase.

1. Introduction

In the search for functional soft materials, liquid crystals (LCs) are singular examples in which molecular units self-assemble by means of non-covalent interactions in controlled organizations at the nanoscale.[1–2] This ability, linked to the vast possibilities of molecular design, highlights their great potential to develop novel stimuli-responsive materials.[3–5] Self-assembly that provide LC order may also manifest in other types of soft materials, such as in molecular gels.[6] Nevertheless, combined studies on molecules with dual LC and gel behavior to help rationalize the design of soft materials from the nano to the macroscale are scarce.[7–8]

Dendritic structures own excellent characteristics for the self-assembly in LC phases[9–10] or gels.[11–13] This is because dendrimers and dendrons are regularly branched polymers with vast possibilities of functionalization at their different regions (apex or focal point, dendritic middle region, periphery) boosting intermolecular interactions within a controlled structure.[14–15] In this respect, a few dendrimers[16–21] and dendrons[22–24] are reported to show both LC and gel behaviors.

From the variety of dendritic structures, poly(benzyl ether) dendrons with terminal long chains (Percec-type dendrons) are reported to self-assemble into complex systems with cylindrical or spherical shapes mimicking natural nanostructures, like the ones found in viruses.[25–27] These assemblies are related with columnar or cubic LC phases, and they have been found in poly (benzyl ether) dendrons with varied focal points such as carboxylic acids,[28–30] methyl esters,[28,30] metal carboxylates, [29] alcohols,[28,30–32] aminoacids,[33] crown ethers,[30,34] oligo(ethylene) oxide;[29,35] phenol,[36] disulfide,[37] carbaldehyde,[32] fullerene,[32] carbazole[38] or pyrene[39–40] derivatives; or precursory groups for dendronized polymers such as styrene or methacrylate.[41] On the other hand, organogel behavior has been described with dipeptides at their apex. [42–43] Not only the dendritic structure, but also the functional apex is important to modulate the supramolecular interactions involved in the assembly process of these monodendrons.[30].

This behavior makes the referred dendrons highly appealing for stimuli-responsive soft materials. In particular, light emission can be combined with anisotropy, fluidity and self-healing properties of the LC phase, or either be influenced by the sol–gel transition of molecular gels. In this way the luminescence of the soft material can respond upon changes in the molecular assembly.[44–46] Unfortunately, many classical luminophores quench their emission in their aggregated state at high concentrations or in the solid

---

* Corresponding authors.
E-mail addresses: rgimenez@unizar.es, raquel.gimenez@csic.es (R. Giménez).

https://doi.org/10.1016/j.molliq.2022.120109
0167-7322/© 2022 The Authors. Published by Elsevier B.V.

state, which made not feasible to attain this property. In order to avoid the undesired quenching, there are some molecular structures that show the opposite effect, called “Aggregation-Induced Emission“ AIE,[47–48] that is the increase of luminescence upon aggregation. Despite the AIE effect has been documented in LCs, it has not been studied in LC dendrons.[49].

Among different photoluminescent (PL) platforms, 4-aryl-3,5-dimethyl-1*H*-pyrazole combines hydrogen bonding abilities[50] with AIE characteristics in soft matter.[51–52] The inclusion of pyrazole at the apex of a dendritic structure, albeit unexplored, should be feasible to obtain supramolecular LC and gels that potentiate their luminescence in the aggregated state. Here it is reported the synthesis, self-assembly and PL properties of these novel pyrazole dendrons incorporating different structural variations, among them two different linkers (amide or ether series, Fig. 1) in order to further modulate the supramolecular interactions and to analyze the influence on the properties. A combined study of NMR, IR and X-ray diffraction in the LC and gel states is performed aiming at establishing analogies between these two classes of soft materials.

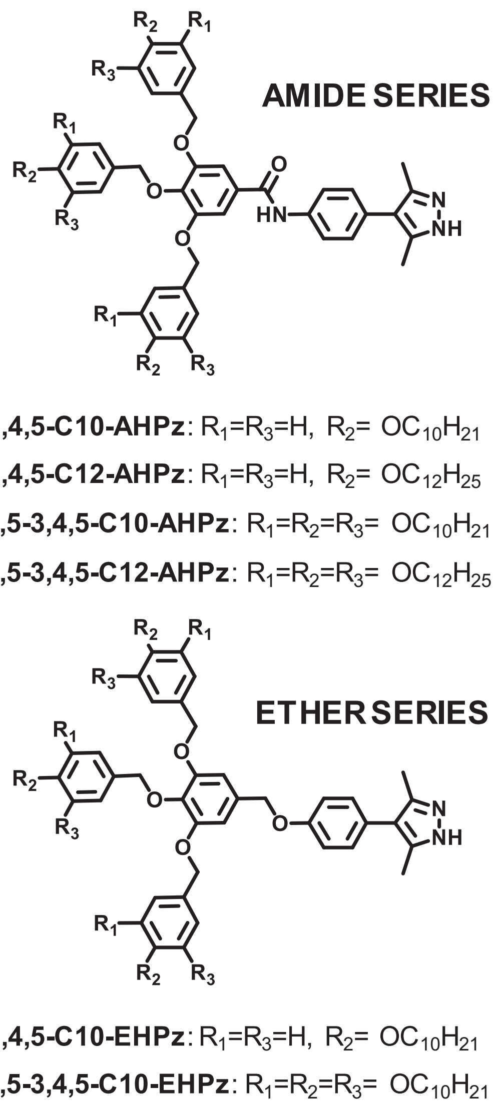

4-3,4,5-C10-AHPz: $R_1=R_3=H$, $R_2= OC_{10}H_{21}$

4-3,4,5-C12-AHPz: $R_1=R_3=H$, $R_2= OC_{12}H_{25}$

3,4,5-3,4,5-C10-AHPz: $R_1=R_2=R_3= OC_{10}H_{21}$

3,4,5-3,4,5-C12-AHPz: $R_1=R_2=R_3= OC_{12}H_{25}$

4-3,4,5-C10-EHPz: $R_1=R_3=H$, $R_2= OC_{10}H_{21}$

3,4,5-3,4,5-C10-EHPz: $R_1=R_2=R_3= OC_{10}H_{21}$

Fig. 1. Chemical structures of the dendronized pyrazoles studied in this work.

2. Results and discussion

2.1. Synthesis and characterization

Pyrazole dendrons were synthesized by modification of the apex of dendronized benzoic acids or benzyl alcohols following Scheme S1. All experimental procedures and characterization data are collected in the Supporting Information file. Amide series were prepared by an amidation reaction of the precursory dendritic acids with 4-(4-aminophenyl)-3,5-dimethyl-1*H*-pyrazole using *N*,*N*-dicyclohexylcarbodiimide (DCC) and (dimethylamino)pyridinium *p*-toluenesulfonate (DPTS). Ether series were prepared by reacting dendritic benzyl alcohols with 3-(4-hydroxyphenyl)-2,4-propanodione by Mitsunobu reaction, and subsequent synthesis of the heterocycle using hydrazine hydrate. Chemical structures were confirmed by NMR, mass spectrometry and elemental analysis.

^{1}H NMR spectra also allow us to extract information about the structure of the dendrons in solution, by analyzing the signals corresponding to the methylenoxy protons (3.5–4 ppm).[28] In this region 4–3,4,5-substituted dendrons show two superimposed triplets in a relationship 4:2 in both series. These spectra are in accordance with a free rotation of the benzyloxy groups in a flat-wedge conformation of the dendron (Fig. 2a). On the other hand, for the 3,4,5–3,4,5-substituted dendrons of both series ^{1}H NMR spectra show a multiplet, and a triplet at higher fields in a relationship 14:4 (Fig. 2b). This triplet (3.76 ppm) belongs to Hr’’’ and the shift to higher fields is due to the fact that Hr’’’ is close to the anisotropic shift region of the phenyl rings in 3,5 positions, suggesting a bulky cone conformation.[28] Thus, regardless of the series, dendrons with three terminal chains have a wedge-shaped conformation and dendrons with nine terminal chains exist as a cone conformation. In addition, as Hr’’ signals belonging to the outer rings appear for 3,4,5–3,4,5-C10-EHPz at slightly higher fields (3.87 ppm) than for the corresponding amide compound 3,4,5–3,4,5-C10-AHPz (3.88 ppm), the ether compound seems to be in a bulkier cone conformation than the amide analogue.

2.2. Self-assembly in bulk: LC behavior

The thermal stability of the compounds was analyzed by thermogravimetric analysis (TGA) and their mesomorphic properties studied by polarized optical microscopy (POM), differential scanning calorimetry (DSC) and X-ray diffraction (XRD). All synthesized dendrons show high thermal stability and LC behavior, and this is independent of the number of terminal chains or their length (C10 or C12). In general, amide series show higher transition temperatures than those of the corresponding ether compounds as consequence of their ability to establish additional hydrogen bonds. Main differences in their thermal behavior come from the number of terminal chains (Tables 1 and S1). Microphotographs of the mesophases, DSC thermograms and XRD images are shown in Fig. 3 and Figs. S1-S3.

C10 dendrons with 4–3,4,5- substitution are semicrystalline materials and show enantiotropic Col_h mesophases, with clearing points higher for the amide compounds 4–3,4,5-C10-AHPz (130 °C) and 4–3,4,5-C12-AHPz (134 °C) than for the ether analogue 4–3,4,5-C10-EHPz (85 °C). A glass transition (T_g) is observed in the subsequent cooling/heating cycles, corresponding to a vitrification of the Col_h as consequence of the loss of conformational freedom of the alkyl tails, keeping the hexagonal order at room temperature (glassy Col_h or $Col_{h(g)}$). A longer length of the terminal chains (going from C10 to C12) does not favor the LC properties as the melting point increases. However, the LC temperature range is

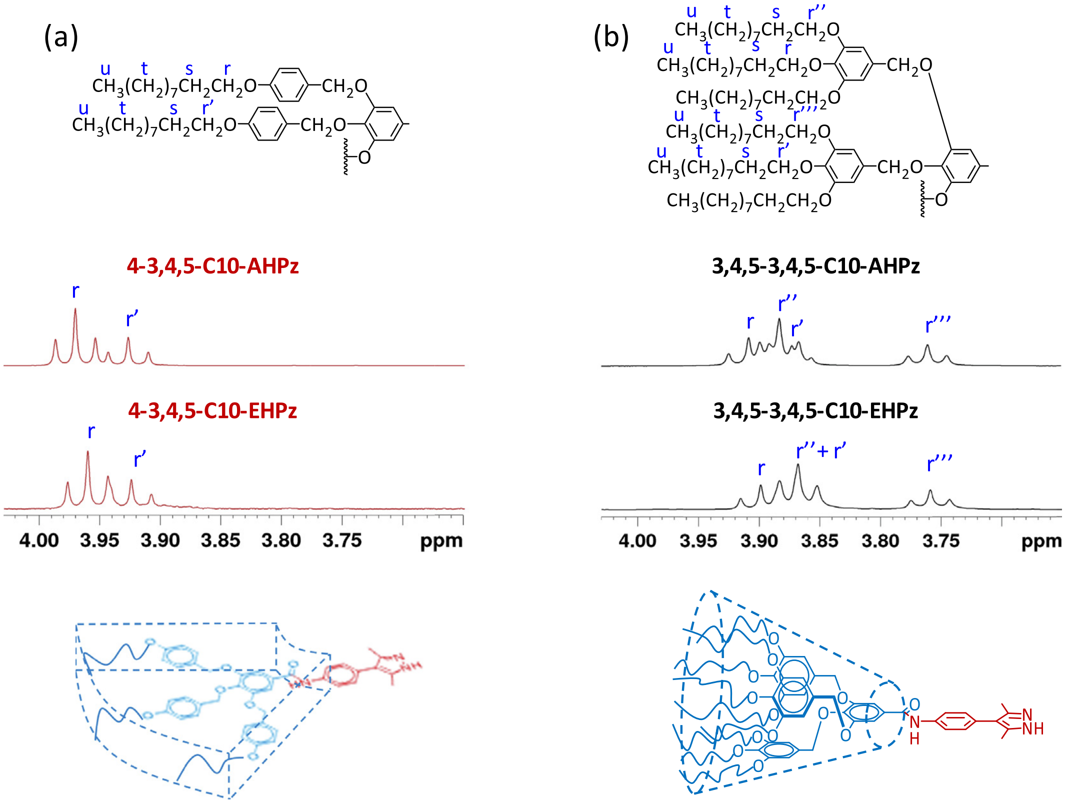

Fig. 2. ^{1}H NMR signals in the region of methylenoxy protons of a) 4–3,4,5-substituted compounds. See at the bottom a representation of the wedge-shaped conformation for amide series. b) 3,4,5–3,4,5-substituted compounds. See at the bottom a representation of the cone-shaped conformation for amide series.

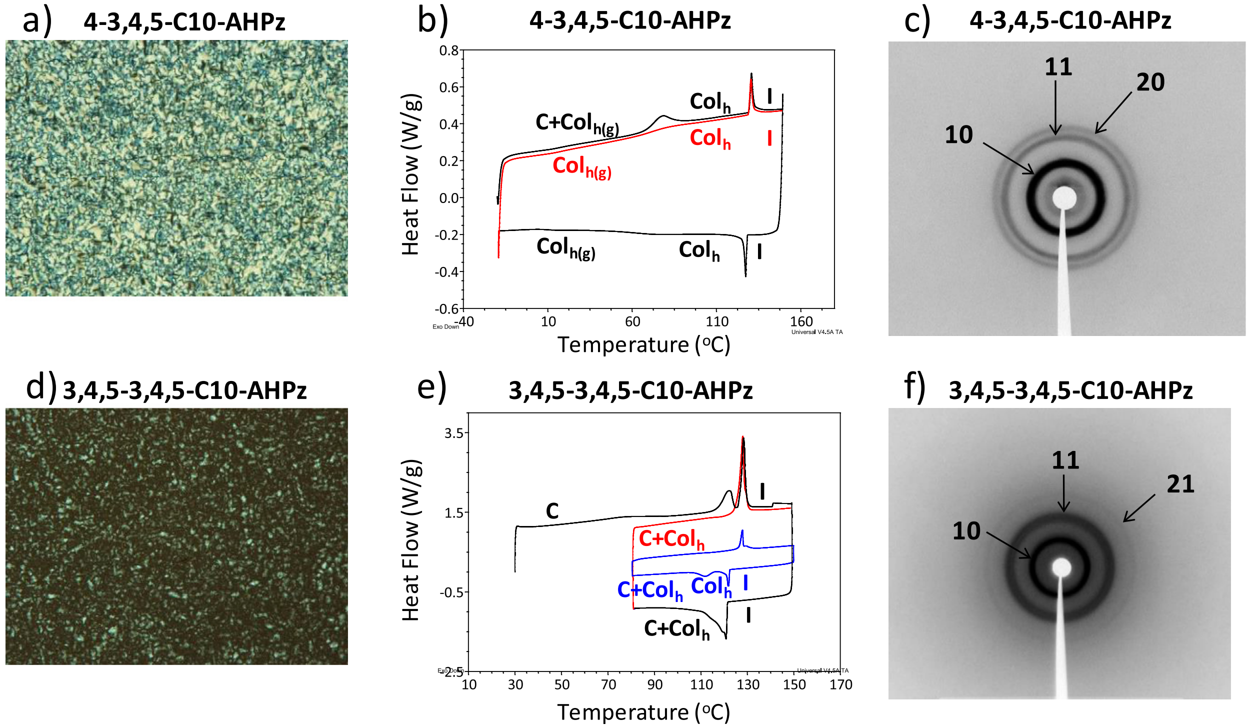

Fig. 3. Textures of the mesophases observed at POM on cooling at 98 °C (a), or at 90 °C (d). DSC traces (b,e, black: 1st cycle at 10 °C min^{-1}, red: 2nd cycle 10 °C min^{-1}, blue: cycle at 2 °C min^{-1}). XRD diffractograms (low angle region) at 20 °C (c) and 125 °C (f). (For interpretation of the references to colour in this figure legend, the reader is referred to the web version of this article.)

the same (59 °C) for both compounds on second heating after vitrification.

An increase in the number of terminal chains of the dendron from three to nine favors crystallization. Thus, 3,4,5–3,4,5-substituted dendrons are crystalline solids that melt directly to isotropic liquid and show the LC phase only on cooling (monotropic mesophase). Moreover, the LC phase is quite unstable upon cooling and partially crystallizes in the cooling cycle and successive heating cycles, being the crystallization faster for amide series than for the ether series. Nevetherless, XRD experiments performed at high temperatures arise diffractograms compatible with a hexagonal columnar phase (see below). For this substitution an increase in the length of the terminal chains from C10 to C12 does not have a relevant effect on the thermal behavior.

XRD diffractograms of the LC phases are compatible with columnar mesophases with hexagonal symmetry for all compounds. In all diffractograms a diffuse halo at high angles corresponding to an average distance of 0.46 nm typical of LC phases is observed. In addition, several reflections in a reciprocal relationship characteristic of a hexagonal lattice were measured at small angles (Table S2, Fig. 3c, f and Fig. S3). In the high angle region only a diffuse halo is observed for all cases, which means the lack of intracolumnar order, and confirming the LC nature of the phase.

With the information collected from the XRD experiments a model for the supramolecular organization of dendrons in the mesophase is inferred. As explained in the characterization section, a single dendron has a wedge-shape or cone shape in solution, therefore does not meet the characteristics to form a discoid structure as occurs in columnar phases of discotic LCs. However, several non-discoid molecules can aggregate to give a columnar arrangement.

The lattice parameter values (*a* in Table 1) do not substantially change on increasing dendron substitution, and show a slight decrease, pointing to a self-assembly model in cylinders in which several dendrons can be accommodated radially with varied number of dendrons along the cylinder axis. For comparison purposes based on this model, if a reasonable average density value close to 1 g cm^{-3} is assumed, the calculated number of molecules in a cylinder of thickness h = 0.46 nm vary from around six dendrons for the 4–3,4,5-substitution to around three dendrons for the 3,4,5–3,4,5-substitution (Z in Table 1). That is, the number of dendrons decreases with the increased number of peripheral chains. Lattice parameters are similar in both series, being slightly smaller in the ether compound than the analogous amide for the 3,4,5–3,4,5-substitution, and this could be related with the more flexible conformation of the ether compounds.

Cone-shaped dendrons have been described to show cubic phases,[28] complex tetragonal 3D phases,[53] or quasicrystals [54] over the hexagonal columnar phase. Here, cubic or more complex phases have not been observed, although the low stability of the observed mesophases precludes a definite conclusion with the performed experiments.

The formation of hexagonal columnar mesophases from conical dendrons is not frequent, but it has been reported previously by polymerization of conical dendrons reaching high degree of polymerization, which then adopt a cylinder model.[25,41] In the cylinder, it is suggested that the conical dendrons get distorted into a flat wedge-shape that allows a columnar mesophase arrangement.

Here, for the column formation there is a segregation between the bulky apolar dendron periphery and the polar part of the apex, that is the amide and pyrazole groups. This is confirmed in their FTIR spectra, which show that amide and pyrazole groups are engaged in hydrogen bonds. Thus, they show N—H stretching bands of pyrazole (ca 3190 cm^{-1}) and N—H (3280 cm^{-1}) and C═O (1650 cm^{-1}) stretching bands of amide groups in the associated region (Table S3). In the proposed assembly model the molecules interact by hydrogen bonding at their focal points forming a supramolecular polymer, and extend the dendritic backbone radially (Fig. 4).

In view of the PL properties of the focal point, the AIE behavior of the novel dendronized pyrazoles in the obtained assemblies was studied. The PL spectra were recorded in dilute tetrahydrofuran (THF) solutions and in thin films (Table 2). Clear differences were observed depending on the series (Fig. 5).

Amide series show a weak emission band in the UVA region (354–358 nm) in diluted THF by excitation at the absorption maxima. The quantum yield (*QY*) is very low (estimated to be less than 0.1 %). However, in thin film the emission is shifted to the blue region (433–444 nm) and the quantum yield increases two orders of magnitude (about 11–14 %), with no important differences depending on the substitution. Ether series show one emission band in the UVA region in thin film (338–340 nm) similar to the diluted solution, and their quantum yield is much lower (2–3 %). Thus, dendronized pyrazoles show clear differences in PL properties depending on the series, and amide series behave as AIE LCs.

2.3. Self-assembly in solvents: Gel behavior

In order to evaluate the potential of these materials for dual LC/gel behavior, the gel-forming abilities of the dendronized pyrazoles were tested in different solvents at a concentration of 5 wt%. Amide series were found to gel ethyl acetate and low-polar solvents such as dodecane and cyclohexane, whereas ether series gave rise to precipitates in these solvents. In polar solvents such as acetone and ethanol all compounds were non-soluble. Supergelator behavior was found for amide series in cyclohexane as a minimum gelator concentration was found to be below 1 wt%. They were 0.4 wt% for 4–3,4,5-C10-AHPz, 0.5 wt% for 4–3,4,5-C12-AHPz and 0.2 wt% for 3,4,5–3,4,5-C10-AHPz and 3,4,5–3,4,5-C12-AHPz. Overall, the alkyl length does not seem to affect gelation concentration but gelation ability is favored by the increase in alkyl substitution.

Gels in cyclohexane were transparent for 4–3,4,5-substitution and translucent for 3,4,5–3,4,5-substitution. The morphology of the xerogels was studied by POM, SEM and TEM. Birefringent

Table 1
Thermal and XRD data for the pyrazole dendrons.[a]

Compound	T_d (°C)	T_m (°C)	T_g (°C)	T_i (°C)	*a* (nm)	*Z*
4–3,4,5-C10-AHPz	278	78	71	130	5.17	5.8
4–3,4,5-C12-AHPz	282	142	75	134	5.36	5.9
4–3,4,5-C10-EHPz	274	59	44	85	5.18	6.0
3,4,5–3,4,5-C10-AHPz	300	132	–	122	4.95	2.9
3,4,5–3,4,5-C12-AHPz	318	127	–	121	5.31	3.0
3,4,5–3,4,5-C10-EHPz	291	99	20	97	4.86	2.8

[a] T_d: decomposition temperature corresponding to a 5 % weight loss by TGA. T_m: melting point (taken at DSC first heating cycle). T_g: temperature of the transition from a glassy Col$_h$ (Col$_{h(g)}$) to the Col$_h$ mesophase (taken at DSC second heating cycle). T_i: temperature of the transition from a Col$_h$ mesophase to the isotropic liquid. *a*: measured lattice parameter for the Col$_h$ mesophase. *Z*: number of dendrons per columnar stratum of thickness 0.46 nm.

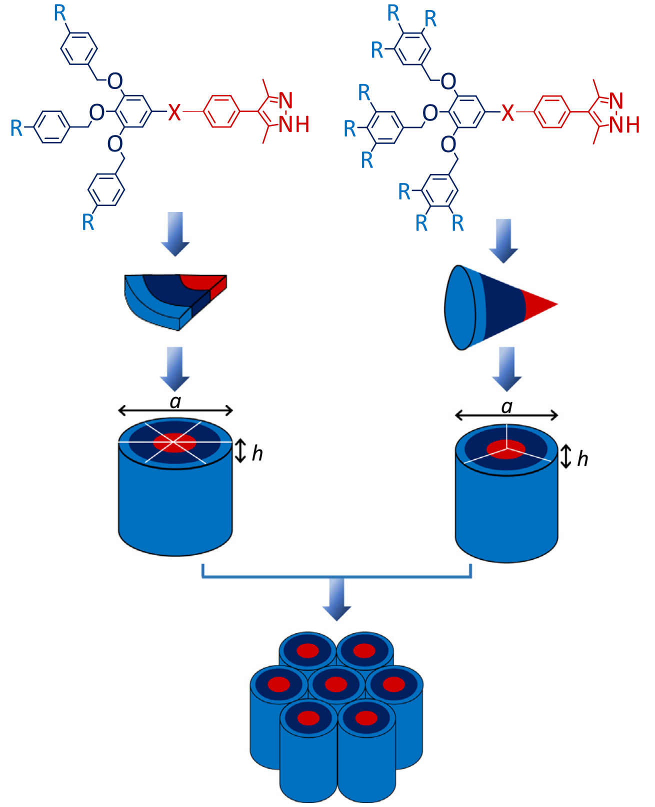

Fig. 4. Model for the self-assembly of the pyrazole dendrons in the LC phase following a cylinder model (wedge-shape and cone-shape represent the conformation of an isolated dendron). This is an idealized model and does not necessarily imply that there are discrete discs of thickness 0.46 nm containing six (or three) molecules. This is an average number and it would also be possible to describe the structure as twice that number, i.e. twelve (or six) molecules, filling a cylinder of height 0.92 nm.

fiber-like areas distributed in the optically isotropic solvent media were observed at POM between crossed polarizers (Fig. 6a–b). Xerogels analyzed by TEM and SEM gave rise to fibrillar networks with a width distribution between 35 and 65 nm, and they were intertwinned forming thicker fibers up to 330 nm width (Fig. 6c–d). TEM studies were carried out at a lower concentration and, even though huge amount of fibers precluded a correct observation, this indicates that fibers exist at very low concentrations.

In addition, gels exhibit a similar light emission to the LC materials, exhibiting a broad emission band in the blue-violet region of the visible spectra, with a maximum around 440 nm. Upon heating there is a change to the sol state observing a decrease in the intensity of the emission while keeping a similar wavelength. This change in emission is more abrupt for the 3,4,5–3,4,5-substitutions (Fig. 6e and Fig. S4). Fig. 6f shows this effect for 3,4,5–3,4,5-C10-AHPz. It is observed that upon initial heating the emission band barely changes. After heating over T_{gel} (45 °C) the material become partially gelled and start to weaken the emission, and between 50 °C and 60 °C a sudden decrease in emission is produced that can be attributed to a break-up of the fibrillar network in the sol state. Upon cooling the sol state at room temperature the gel state does not reform immediately but after 24 h and the luminescence increases upon forming the gel (Fig. S5). This indicates that the compound shows a reversible gel-sol behavior with aggregation-induced emission (AIE), as the increase in emission is not due to the effect of lowering the temperature. The increase is estimated to be significative, about two orders of magnitude. This is particularly desired for functional materials required to be emissive in the aggregated state instead to the commonly found quenching of luminescence. The increase in emission takes place as consequence of fiber formation. A similar effect, consistent with the postulated AIE property, was obtained by comparison with a THF solution which is barely luminescent at 0.5 wt%, the same concentration of gel formation (Fig. S6).

In order to analyze the supramolecular interactions involved in the formation of the cyclohexane gel of 3,4,5–3,4,5-C10-AHPz at 0.5 wt%, the material was studied by IR and NMR spectroscopy. IR spectroscopy allows to evaluate the association mode of the amide and pyrazole functional groups in gel state. For this reason, the IR spectra of the isolated molecules were measured in a dichloromethane solution at 0.5 wt% and compared with the cyclohexane gels at the same concentration (Fig. S7). In dichloromethane the IR spectrum shows a band at 3450 cm^{-1} for the NH stretching and a band at 1678 cm^{-1} for the C=O stretching vibration, characteristic of non-associated amide groups. However, the IR spectrum of the gel state shows bands at 3257 cm^{-1} and 1642 cm^{-1}, indicating that the amide group is associated by hydrogen bonding. Moreover, a band around 3170 cm^{-1} is also observed, and this indicates that the NH of pyrazole is also involved in hydrogen bonds.

^{1}H NMR spectra at room temperature show only a few broad signals (Fig. 7a). This is a typical behavior for gels, where the extended supramolecular network reduces significantly the mobility of the molecules and the observed signals are due to some isolated molecules or small aggregates in solution [55].

On heating it is observed an increase in resolution, thus, the signals corresponding to the aromatic protons, the methylene groups close to the phenyl rings and the methyl substituents of the pyrazole ring sharpen and shift toward lower fields. This indicates a decrease of the π-stacking that gives a deshielding of protons with temperature. Aromatic protons closer to the amide group and the amide NH proton shift in the opposite direction, which is explained by the breakage of the hydrogen bonds by increasing temperature. The greatest variation is observed for the amide NH proton, which changes from 8.24 to 7.55 ppm. This indicates that the gel also stablishes hydrogen bonding interactions between the closest dendrons.

The ^{1}H NMR study allows to observe that the temperature at which the spectra starts to be resolved is in agreement with the temperature at which the luminescence drops (Fig. 6e), consistent to be due to the breakage of the gel architecture.

To study further the self-assemblies that give rise to this kind of gels a Saturation Transfer Difference (STD) NMR experiment was performed. This technique has been used to propose interaction models for the molecules in the gel state.[56–57] STD spectra show signals for all protons (Fig. 7b), demonstrating the existence of a

Table 2
UV–vis and PL data.

Compound	λ_{abs}^{THF} (nm)	λ_{em}^{THF} (nm)	λ_{em}^{film} (nm)	QY^{film} (%)
4–3,4,5-C10-AHPz	283, 300^{sh}	356	442	11
4–3,4,5-C12-AHPz	285, 303^{sh}	354	441	12
4–3,4,5-C10-EHPz	275, 282	336	338	2
3,4,5–3,4,5-C10-AHPz	286	354	441	14
3,4,5–3,4,5-C12-AHPz	289	355	444	11
3,4,5–3,4,5-C10-EHPz	281	334	340	3

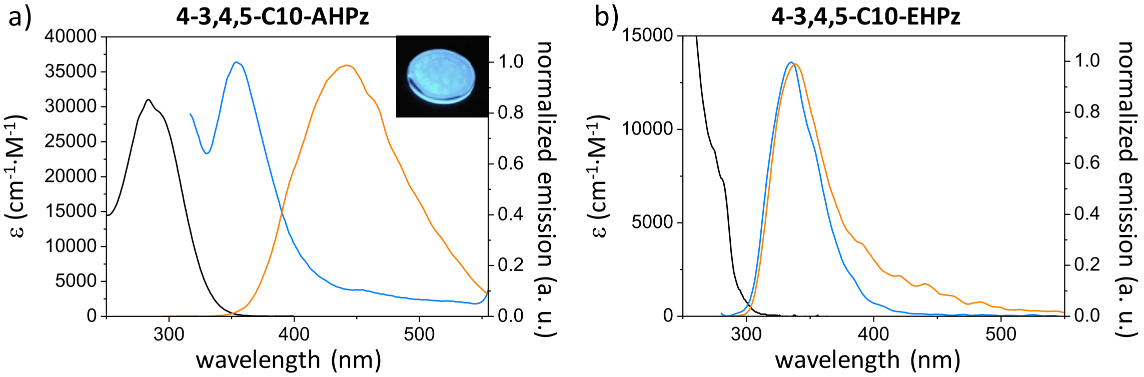

Fig. 5. UV–vis absorption spectra in 10^{-5} M THF solution (black line), PL spectra in 10^{-6} M THF solution (blue line) and PL spectra of a LC thin film (orange line) for a) 4–3,4,5-C10-AHPz and b) 4–3,4,5-C10-EHPz. Inset: thin film irradiated with a UVA lamp (365 nm). (For interpretation of the references to colour in this figure legend, the reader is referred to the web version of this article.)

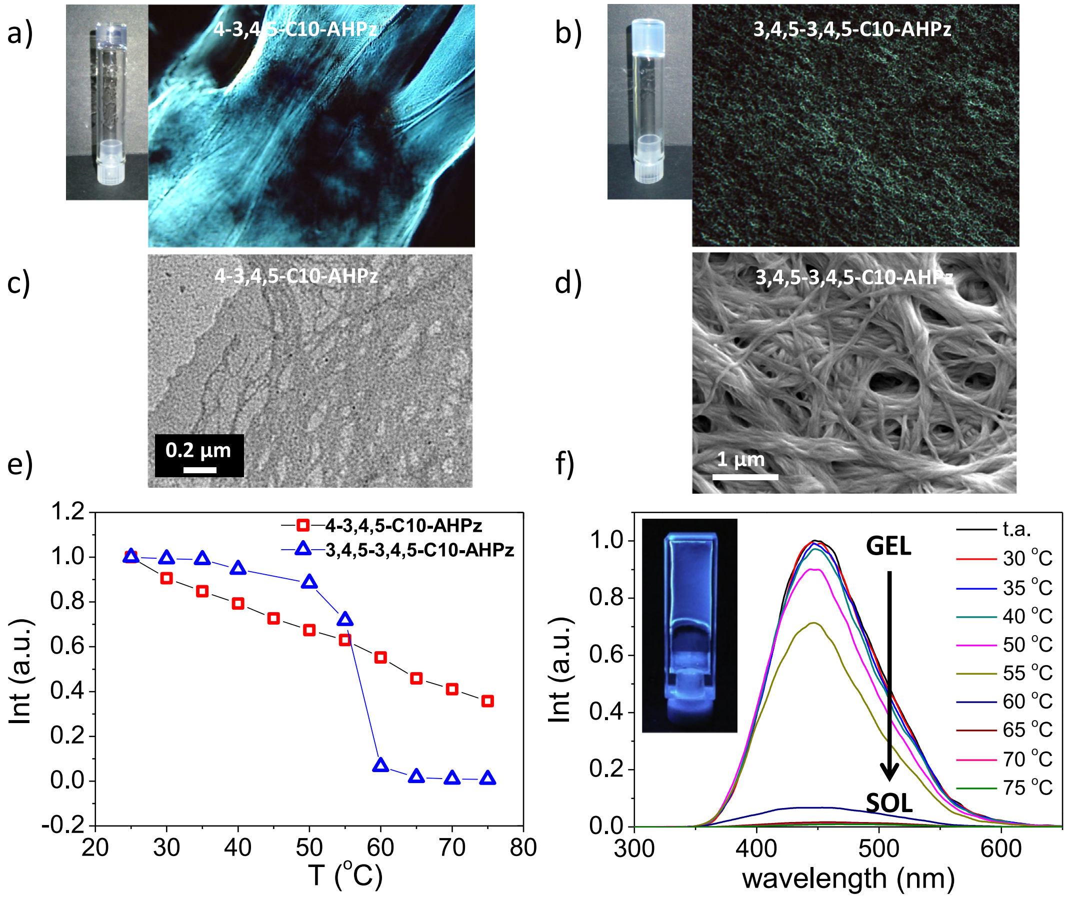

Fig. 6. Gels in cyclohexane at 0.5 wt%:a-b) microphotographs under polarized light, c) TEM image, d) SEM image, e) variation of PL intensity with increased temperature, f) PL spectral changes upon heating the 3,4,5–3,4,5-C10-AHPz gel to the sol state, and picture of the gel irradiated with a UVA lamp (365 nm).

rigid matrix that allows the magnetization transfer to be possible. The maximum STD signal was found for the methyl signals (Ha), followed by the closest aromatic protons to the pyrazole ring He, Hf and Hk. Weaker STD signals were observed for the benzyl protons and the aromatic protons of the outer phenyl rings. This suggests that the aromatic part of the poly(benzyl)ether dendron is less exposed to form intermolecular interactions in the gel structure, probably due to a cone conformation. The solvent signal also shows STD signal so the molecules of solvent also play a role in the gel structure, probably by intercalation with the outer hydrophobic tails.

On the other hand, NOESY experiments have been also carried out to collect information on the gelation process. Due to the low concentration of mobile molecules in the gel, the only information provided is that all the cross peaks are negative (slow rotational tumbling), which supports the existence of supramolecular structures in exchange with the rigid matrix gel (Fig. S8).

In order to study if there exists any mesoscopic organization in the gel fibers a XRD study was tried for higher concentration cyclohexane gels (5 wt%). The obtained diffractograms (Fig. S9) show two maxima in the low angle region that can be indexed to a 2D hexagonal lattice (Table S4). These maxima are very weak, which

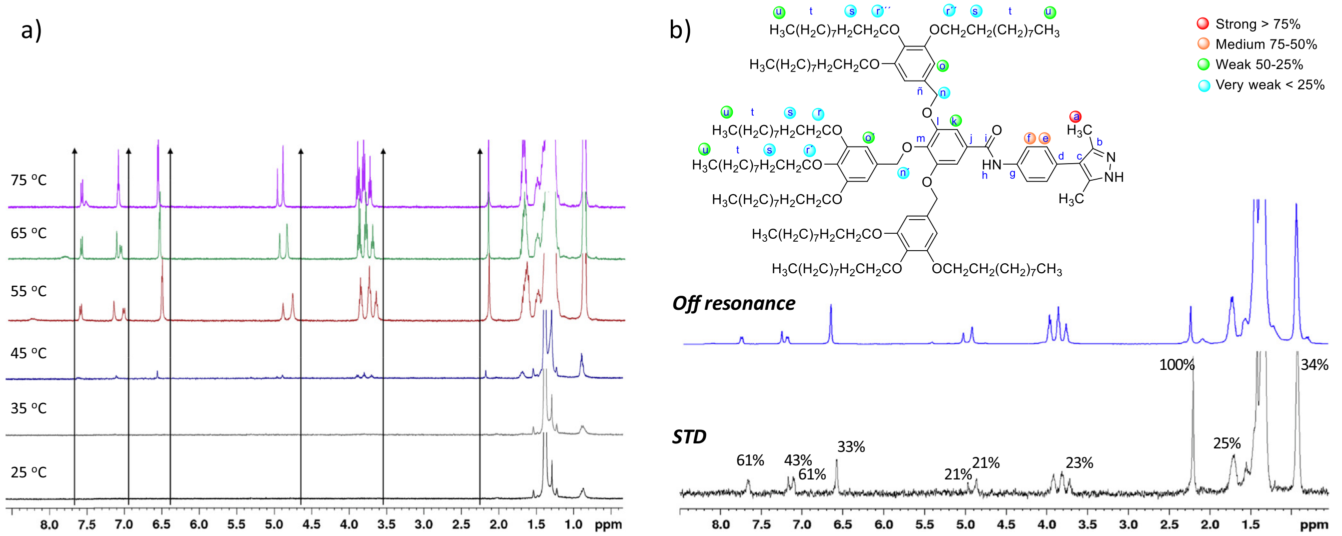

Fig. 7. ^{1}H NMR spectra of 3,4,5–3,4,5-C10-AHPz in cyclohexane d_{12}, 0.5 wt%. a) at variable temperature. b) Overlay of off-resonance (blue) and STD (black) spectra at 325 K and their corresponding percentage of STD according to the assignment depicted in the structure above. (For interpretation of the references to colour in this figure legend, the reader is referred to the web version of this article.)

can be due to the low gelator content in the materials. Moreover, in the high angle region a diffuse halo is observed at 0.46 nm, and this is related to the scattering of solvent molecules trapped in the gel network and the alkyl tails of the dendrons in a conformational disordered state. The existence of Bragg reflections in the gel at 5 wt% allows to investigate molecular order in the single fibres, which then pack to form larger bundles. From these data we infer that gel exhibits a similar hexagonal columnar organization to the LC phase found in bulk. The network parameter of the gels are larger than for the LC phase, e.g. for 3,4,5–3,4,5-C10-AHPz is a = 6.04 nm in gel state vs a = 5.31 nm in the LC phase. An estimation of the number of molecules similar to previously done considering a columnar stratum of thickness 0.46 nm, and supposing that the density of the material is about 0.78 g cm^{-3} (cyclohexane density), yields that the number of molecules is six or three, similar to the LC phase. Therefore, we propose a similar organization to the LC Col$_h$ phase but here the solvent would be also interacting with the peripheral alkyl tails making larger the lattice parameter.

In this model, and similarly to the organization schematized in Fig. 4 for the LC phases, dendrons interact at their apex allowing hydrogen bonding between amide and pyrazole groups in such a way that six or three dendrons give rise to a cylindrical structure formed by a polar core and alkyl tails and solvent at the periphery. This stratum propagates and associates with other columns giving rise to fibrils that form fibers whose network is able to efficiently entrap cyclohexane molecules forming the gel. Moreover, this gel assembly is able to enhance luminescence by two orders of magnitude.

3. Conclusions

This work unprecendentedly shows the rich self-assembly behavior obtained by grafting a pyrazole-derived platform at the focal point of poly(benzyl ether) dendrons. These dendrons are novel pyrazole LCs.[58] Moreover, the selected pyrazole-derived groups promote LC behavior with AIE properties, and extend similar mesoscale self-assembly in gels.

By analyzing different structural variations at the dendritic scaffold it is observed that, depending on the number of terminal chains, wedge-shaped of cone-shaped conformations are obtained in solution. In this respect, the novel pyrazole-based focal point exhibits great tendency to arrange dendrons of both conformations in columnar mesophases. In the mesophase, the non-discoid entities aggregate in cylindrical assemblies in which the focal points interact by hydrogen bonding in the inner region. Similarly, dendrons form supramolecular polymers by hydrogen bonding with similar organization to the LC state in cyclohexane gels.

Amide linker between the focal point and the dendritic scaffold show better performance than the most commonly used ether linker in poly(benzyl ether) dendrons. Thus, amide series stabilizes LC behavior and induces supergel behavior, in addition to AIE and a luminescence shift from the UVA region to the blue part of the visible region, with similar behavior in both LC and gels.

These results showcase that the self-assembly of dendrons in LC phases can be extended to the organization in solvents for the development of novel stimuli-responsive soft matter that is able to exhibit luminescence changes depending on the sol–gel or aggregated states.

Funding sources

This work was supported by Spanish Government projects PGC2018-093761-B-C31, PGC2018-097583-B-100 (MCIU/AEI/FEDER, UE), Agencia Estatal de Investigación PID2020-119512GB-I00 (Spain); the Gobierno de Aragón/FSE (research groups E47_20R and E50_20D), and Industrias Químicas del Ebro (IQE) (Cátedra IQE, Universidad de Zaragoza).

Data availability

Research data included in the supporting information file

Declaration of Competing Interest

The authors declare that they have no known competing financial interests or personal relationships that could have appeared to influence the work reported in this paper.

Acknowledgements

We thank Spanish Government projects PGC2018-093761-B-C31, PGC2018-097583-B-100 (MCIU/AEI/FEDER, UE), Agencia Estatal de Investigación PID2020-119512GB-I00 (Spain); the Gobierno de Aragón/FSE (research groups E47_20R and E50_20D), and Industrias Químicas del Ebro (IQE) (Cátedra IQE, Universidad de Zaragoza) for financial support. We thank Dr. O. Crespo for assistance with *QY* measurements. We also acknowledge the use of "Servicios Científico-Técnicos" of CEQMA (CSIC), Servicio General de Apoyo a la Investigación – SAI and Laboratorio de Microscopías Avanzadas (LMA), Universidad de Zaragoza.

Appendix A. Supplementary material

A supplementary information file contains Materials and Methods. Synthetic details. ^1H and ^{13}C NMR spectra. POM, DSC and XRD data for LC phases. PL, IR, NOESY spectrum and XRD data for gels (PDF). Supplementary data to this article can be found online at https://doi.org/10.1016/j.molliq.2022.120109.

References

[1] P.J. Collings, Liquid Crystals: Nature's Delicate Phase of Matter, 2nd edition., Princeton University Press, Princeton, 2002.
[2] H.K. Bisoyi, Q. Li, Liquid crystals: versatile self-organized smart soft materials, Chem. Rev. 122 (2022) 4887.
[3] T. Kato, J. Uchida, T. Ichikawa, B. Soberats, Functional liquid-crystalline polymers and supramolecular liquid crystals, Polym. J. 50 (2018) 149.
[4] T. Kato, J. Uchida, T. Ichikawa, T. Sakamoto, Functional liquid crystals towards the next generation of materials, Angew. Chem. Int. Ed. 57 (2018) 4355.
[5] S.J.D. Lugger, S.J.A. Houben, Y. Foelen, M.G. Debije, A.P.H.J. Schenning, D.J. Mulder, Hydrogen-bonded supramolecular liquid crystal polymers: smart materials with stimuli-responsive, self-healing, and recyclable properties, Chem. Rev. 122 (2022) 4946.
[6] R.G. Weiss, The past, present, and future of molecular gels. What is the status of the field, and where is it going?, J Am. Chem. Soc. 136 (2014) 7519.
[7] M. Castillo-Vallés, A. Martínez-Bueno, R. Giménez, T. Sierra, M.B. Ros, Beyond liquid crystals: new research trends for mesogenic molecules in liquids, J. Mater. Chem. C 7 (2019) 14454.
[8] K. Steck, S. Dieterich, C. Stubenrauch, F. Giesselmann, Surfactant-based lyotropic liquid crystal gels – the interplay between anisotropic order and gel formation, J. Mater. Chem. C 8 (2020) 5335.
[9] S. Hernández-Ainsa, M. Marcos, J.L. Serrano, Dendrimeric and Hyperbranched Liquid Crystal Structures, in: J.W. Goodby, P.J. Collings, T. Kato, C. Tschierske, H.F. Gleeson, P. Raynes (Eds.), Handbook of Liquid Crystals, 7, Wiley-VCH, Weinheim, 2014, pp. 259–300.
[10] B. Donnio, S. Buathong, I. Bury, D. Guillon, Liquid crystalline dendrimers, Chem. Soc. Rev. 36 (2007) 1495.
[11] Y. Feng, Y.-M. He, Q.-H. Fan, Supramolecular organogels based on dendrons and dendrimers, Chem. Asian J. 9 (2014) 1724.
[12] J. Matraszek, E. Gorecka, J. Mieczkowski, M. Hejko, D. Pociecha, Hierarchical structures formed by flexible dendrimeric molecules based on gallic acid, Macromol. Chem. Phys. 218 (2017) 1700316.
[13] Y. Feng, Z.-X. Liu, H. Chen, Q.-H. Fan, Functional supramolecular gels based on poly(benzyl ether) dendrons and dendrimers, Chem. Commun. 58 (63) (2022) 8736–8753.
[14] J.M.J. Fréchet, D.A. Tomalia, Dendrimers and Other Dendritic Polymers, Wiley-VCH, Weinheim, Germany, 2001.
[15] G.R. Newkome, C.N. Moorefield, F. Vögtle, Dendrimers and Dendrons: Concepts, Syntheses, and Perspectives, Wiley-VCH, Weinheim, Germany, 2001.
[16] G. Kuang, Y. Ji, X. Jia, E. Chen, M. Gao, J. Yeh, Y. Wei, Supramolecular self-assembly of dimeric dendrons with different aliphatic spacers, Chem. Mater. 21 (2009) 456.
[17] A. Pérez, J.L. Serrano, T. Sierra, A. Ballesteros, D. de Saá, J. Barluenga, Control of self-assembly of a 3-hexen-1,5-diyne derivative: toward soft materials with an aggregation-induced enhancement in emission, J. Am. Chem. Soc. 133 (2011) 8110.
[18] C. Romero-Nieto, M. Marcos, S. Merino, J. Barberá, T. Baumgartner, J. Rodríguez-López, Room temperature multifunctional organophosphorus gels and liquid crystals, Adv. Funct. Mater. 21 (2011) 4088.
[19] I. Gracia, J.L. Serrano, J. Barberá, A. Omenat, Functional organogelators formed by liquid-crystal carbazole-containing bis-MPA dendrimers, RSC Adv. 6 (2016) 39734.
[20] Y. Chen, Y. Lv, Y. Han, B. Zhu, F. Zhang, Z. Bo, C.-Y. Liu, Dendritic effect on supramolecular self-assembly: organogels with strong fluorescence emission induced by aggregation, Langmuir 25 (2009) 8548.
[21] V. Percec, M. Peterca, M.E. Yurchenko, J.G. Rudick, P.A. Heiney, Thixotropic twin-dendritic organogelators, Chem. Eur. J. 14 (2008) 909.
[22] G.-C. Kuang, Y. Ji, X.-R. Jia, Y. Li, E.-Q. Chen, Y. Wei, Self-Assembly of amino-acid-based dendrons: organogels and lyotropic and thermotropic liquid crystals, Chem. Mater. 20 (2008) 4173.
[23] G.-C. Kuang, X.-R. Jia, M.-J. Teng, E.-Q. Chen, W.-S. Li, Y. Ji, Organogels and liquid crystalline properties of amino acid-based dendrons: a systematic study on structure-property relationship, Chem. Mater. 24 (2012) 71.
[24] H. Cheng, H. Gao, T. Wang, M. Xia, X. Cheng, Polycatenar bent-shaped liquid crystals with columnar and cubic phases: Synthesis multi-responsive organogels and chemosensors, J. Mol. Liq. 249 (2018) 723.
[25] V. Percec, C.H. Ahn, G. Ungar, D.J.P. Yeardley, M. Möller, S.S. Sheiko, Controlling polymer shape through the self-assembly of dendritic side-groups, Nature 391 (1998) 161.
[26] B.M. Rosen, C.J. Wilson, D.A. Wilson, M. Peterca, M.R. Imam, V. Percec, Dendron-mediated self-assembly, disassembly, and self-organization of complex systems, Chem. Rev. 109 (2009) 6275.
[27] H.-J. Sun, S. Zhang, V. Percec, From structure to function via complex supramolecular dendrimer systems, Chem. Soc. Rev. 44 (2015) 3900.
[28] V.S.K. Balagurusamy, G. Ungar, V. Percec, G. Johansson, Rational design of the first spherical supramolecular dendrimers self-organized in a novel thermotropic cubic liquid-crystalline phase and the determination of their shape by X-ray analysis, J. Am. Chem. Soc. 119 (1997) 1539.
[29] G. Ungar, V. Percec, M.N. Holerca, G. Johansson, J.A. Heck, Heat-shrinking spherical and columnar supramolecular dendrimers: their interconversion and dependence of their shape on molecular taper angle, Chem. Eur. J. 6 (2000) 1258.
[30] V. Percec, W.-D. Cho, G. Ungar, D.J.P. Yeardley, Synthesis and NaOTf mediated self-assembly of monodendritic crown ethers, Chem. Eur. J. 8 (2002) 2011.
[31] J. Guardià, A. Zare, J. Eleeza, M. Giamberini, J.A. Reina, X. Montané, Synthesis and characterization of dendritic compounds containing nitrogen: monomer precursors in the construction of biomimetic membranes, Sci. Rep. 12 (2022) 1725.
[32] J. Lenoble, N. Maringa, S. Campidelli, B. Donnio, D. Guillon, R. Deschenaux, Liquid-crystalline fullerodendrimers which display columnar phases, Org. Lett. 8 (2006) 1851.
[33] B.M. Rosen, M. Peterca, K. Morimitsu, A.E. Dulcey, P. Leowanawat, A.-M. Resmerita, M.R. Imam, V. Percec, Programming the supramolecular helical polymerization of dendritic dipeptides via the stereochemical information of the dipeptide, J. Am. Chem. Soc. 133 (2011) 5135.
[34] V. Percec, G. Johansson, J. Heck, G. Ungar, S.V. Batty, Molecular recognition directed self-assembly of supramolecular cylindrical channel-like architectures from 6,7,9,10,12,13,15,16-octahydro-1,4,7,10,13-pentaoxabenzocyclopentadecen-2-ylmethyl 3,4,5-tris(p-dodecyloxybenzyloxy)benzoate, J. Chem. Soc., Perkin Trans. 1 (1993) 1411.
[35] V. Percec, D. Schlueter, G. Ungar, S.Z.D. Cheng, A. Zhang, Hierarchical control of internal superstructure, diameter, and stability of supramolecular and macromolecular columns generated from tapered monodendritic building blocks, Macromolecules 31 (1998) 1745.
[36] S. Lecommandoux, H.-A. Klok, M. Sayar, S.I. Stupp, Synthesis and self-organization of rod–dendron and dendron–rod–dendron molecules, J. Polym. Sci., Part A: Polym. Chem. 41 (22) (2003) 3501–3518.
[37] S. Frein, J. Boudon, M. Vonlanthen, T. Scharf, J. Barberá, G. Süss-Fink, T. Bürgi, R. Deschenaux, Liquid-crystalline thiol- and disulfide-based dendrimers for the functionalization of gold nanoparticles. preliminary communication, Helv. Chim. Acta 91 (2008) 2321.
[38] V. Iguarbe, J. Barberá, J.L. Serrano, Functional Janus dendrimers containing carbazole with liquid crystalline, optical and electrochemical properties, Liq. Cryst. 47 (2019) 301.
[39] A. Pitto-Barry, N.P.E. Barry, O. Zava, R. Deschenaux, B. Therrien, Encapsulation of pyrene-functionalized poly(benzyl ether) dendrons into a water-soluble organometallic cage, Chem. Asian J. 6 (2011) 1595.
[40] Y. Shibuya, Y. Itoh, T. Aida, Columnar liquid crystalline assembly of a U-shaped molecular scaffold stabilized by covalent or noncovalent incorporation of aromatic molecules, J. Polym. Sci., Part A: Polym. Chem. 57 (3) (2019) 342–351.
[41] V. Percec, C.H. Ahn, W.D. Cho, A.M. Jamieson, J. Kim, T. Leman, M. Schmidt, M. Gerle, M. Möller, S.A. Prokhorova, S.S. Sheiko, S.Z.D. Cheng, A. Zhang, G. Ungar, D.J.P. Yeardley, Visualizable cylindrical macromolecules with controlled stiffness from backbones containing libraries of self-assembling dendritic side groups, J. Am. Chem. Soc. 120 (1998) 8619.
[42] W.-D. Jang, D.-L. Jiang, T. Aida, Dendritic physical gel: hierarchical self-organization of a peptide-core dendrimer to form a micrometer-scale fibrous assembly, J. Am. Chem. Soc. 122 (2000) 3232.
[43] W.-D. Jang, T. Aida, Dendritic physical gels: structural parameters for gelation with peptide-core dendrimers, Macromolecules 36 (2003) 8461.
[44] S. Yamane, K. Tanabe, Y. Sagara, T. Kato, Stimuli-responsive photoluminescent liquid crystals, Top. Curr. Chem. 318 (2012) 395.
[45] Y. Sagara, S. Yamane, M. Mitani, C. Weder, T. Kato, Mechanoresponsive luminescent molecular assemblies: an emerging class of materials, Adv. Mater. 28 (2016) 1073.
[46] C.D. Jones, J.W. Steed, Gels with sense: supramolecular materials that respond to heat, light and sound, Chem. Soc. Rev. 45 (2016) 6546.
[47] J. Mei, N.L.C. Leung, R.T.K. Kwok, J.W.Y. Lam, B.Z. Tang, Aggregation-induced emission: together we shine, united we soar!, Chem Rev. 115 (2015) 11718.
[48] F. Würthner, Aggregation-Induced Emission (AIE): a historical perspective, Angew. Chem. Int. Ed. 59 (34) (2020) 14192–14196.
[49] J. Voskuhl, M. Giese, Mesogens with aggregation-induced emission properties: Materials with a bright future, Aggregate 3 (2022) e124.
[50] S. Moyano, B. Diosdado, L. San Felices, A. Elduque, R. Giménez, Structural diversity of hydrogen-bonded 4-Aryl-3,5-Dimethylpyrazoles for supramolecular materials, Materials 14 (2021) 4550.

[51] S. Moyano, J. Barberá, B.E. Diosdado, J.L. Serrano, A. Elduque, R. Giménez, Self-assembly of 4-aryl-1H-pyrazoles as a novel platform for luminescent supramolecular columnar liquid crystals, J. Mater. Chem. C 1 (2013) 3119.
[52] S. Moyano, J.L. Serrano, A. Elduque, R. Giménez, Self-assembly and luminescence of pyrazole supergelators, Soft Matter 8 (2012) 6899.
[53] G. Ungar, Y. Liu, X. Zeng, V. Percec, W.-D. Cho, Giant supramolecular liquid crystal lattice, Science 299 (2003) 1208.
[54] X. Zeng, G. Ungar, Y. Liu, V. Percec, A.E. Dulcey, J.K. Hobbs, Supramolecular dendritic liquid quasicrystals, Nature 428 (2004) 157.
[55] G. Yu, X. Yan, C. Han, F. Huang, Characterization of supramolecular gels, Chem. Soc. Rev. 42 (2013) 6697.
[56] V. Lozano, R. Hernández, A. Ardá, J. Jiménez-Barbero, C. Mijangos, M.-J. Pérez-Pérez, An asparagine/tryptophan organogel showing a selective response towards fluoride anions, J. Mater. Chem. 21 (2011) 8862.
[57] S. Debnath, S. Roy, Y.M. Abul-Haija, P.W.J.M. Frederix, S.M. Ramalhete, A.R. Hirst, N. Javid, N.T. Hunt, S.M. Kelly, J. Angulo, Y.Z. Khimyak, R.V. Ulijn, Tunable supramolecular gel properties by varying thermal history, Chem. Eur. J. 25 (2019) 7881.
[58] S.Y. Kotian, C.D. Mohan, A.A. Merlo, S. Rangappa, S.C. Nayak, K.M.L. Rai, K.S. Rangappa, Small molecule based five-membered heterocycles: a view of liquid crystalline properties beyond the biological applications, J. Mol. Liq. 297 (2020) 111686.